Journal of Power Sources 211 (2012) 169–172

Contents lists available at SciVerse ScienceDirect

Journal of Power Sources

journal homepage: www.elsevier.com/locate/jpowsour

Short communication

A proof-of-concept lithium/sulfur liquid battery with exceptionally high capacity density

Sheng S. Zhang*, Dat T. Tran

U.S. Army Research Laboratory, Electrochemistry Branch, RDRL-SED-C, Adelphi, MD 20783-1197, USA

ARTICLE INFO

Article history:
Received 29 February 2012
Received in revised form
31 March 2012
Accepted 2 April 2012
Available online 13 April 2012

Keywords:
Lithium/sulfur battery
Sulfur cathode
Polysulfide
Li anode
Cycle life

ABSTRACT

In this communication, we disclose a proof-of-concept lithium/sulfur liquid battery that has exceptionally high capacity density. In such a battery, the cathode consists of a highly porous carbon cloth (CC) as the cathode current collector and a porous sulfur paper as the source of active material. In the first discharge, sulfur is reduced on the CC surface into high order lithium polysulfide (PS), which dissolves into liquid electrolyte and serves as the catholyte of the so-called "Li/S liquid battery". By adopting a $LiNO_3$-contained electrolyte to protect Li anode, the Li/S liquid cell is shown to cycle reversibly between 1.7 V and 2.8 V with an initial capacity of 778 mAh g^{-1} S, corresponding to a capacity density of 10.1 mAh cm^{-2} CC, which could be the highest capacity density among the rechargeable Li/S batteries reported ever. This work reveals that the high capacity density Li/S batteries can be made through a "Li/S liquid cell" by employing a highly porous carbon electrode to accommodate the insoluble sulfur reduction products (Li_2S_2/Li_2S) with appropriate protection of the Li anode.

Published by Elsevier B.V.

Dissolution of lithium polysulfides (PS) has been long known to be the main reason for the low charging efficiency and high self-discharge of rechargeable Li/S batteries due to their "redox shuttle reactions" between sulfur cathode and Li anode [1,2]. In effort to reduce the redox shuttle of PS, overwhelming researches have been focused on the reduction of the PS diffusion out of the sulfur cathode by impregnating sulfur into high surface carbon to form a so-called "sulfur-carbon composite" based on a general idea that the high surface carbon physically adsorbs/traps the dissolved PS [3–17]. For this purpose, the composite usually comprises a large proportion of carbon. Even such, extra carbon still is needed in the electrode fabrication to obtain the necessary electronic conductivity of the sulfur cathode. Therefore, this approach often results in two lows, i.e. low sulfur content in the composition and low sulfur loading in the cathode, which greatly offsets the advantage of the high energy density of Li/S battery. It is noticed that in most cases, the sulfur content in the cathode is not more than 65 wt.% and the sulfur loading is not higher than 2 mg cm^{-2} [4–7,15–21]. Moreover, this approach is fundamentally ineffective since the negative PS anions will be electrically dragged toward the Li anode by the internal electrical filed in the discharge process. On the other hand, the dissolution of PS in the electrolyte is essential for the sulfur cathode. Since sulfur and its reduction intermediates/products are neither electronic conductive nor ionic conductive, their reactions on a solid–solid interface are very slow. The "solid–liquid" interface between the carbon and the dissolved PS formed by the dissolution of PS must promote the reaction kinetics of the sulfur cathode. Therefore, early studies on the Li/S batteries were mostly focused on the liquid cell systems [22,23]. Considering the fact that the dissolution of PS in organic electrolytes is inevitable and it is essential for the sulfur cathode, we recently proposed a Li/S liquid cell with an in-situ prepared PS (Li_2S_9) as the catholyte and a porous carbon electrode as the cathode current collector [24]. We have shown that the Li/S liquid cells are superior to the conventional Li/S cells in the terms of specific capacity and cycle life.

Due to the limited solubility of PS in organic electrolyte, extra liquid electrolytes are needed to dissolve the PS for a high capacity Li/S liquid battery. To reduce the amount of liquid electrolyte, in this work we propose a new process for the assembly of rechargeable Li/S liquid cells that have exceptionally high capacity density and similar performance, as compared with the conventional Li/S cells. In our cells, the cathode is composed of a highly porous carbon cloth and a porous sulfur paper, of which the former acts as a cathode current collector and a reservoir of the sulfur discharge products (Li_2S_2 and Li_2S) while the letter serves as a source of the active material. The cell starts with elemental sulfur and then converts into a Li/S liquid cell in the first discharge once the high order PS is formed and dissolved into the liquid electrolyte. In this communication, we report our preliminary results on this proof-of-concept Li/S liquid cell.

* Corresponding author. Tel.: +1 (301) 394 0981; fax: +1 (301) 394 0273.
E-mail address: shengshui.zhang.civ@mail.mil (S.S. Zhang).

0378-7753/$ – see front matter Published by Elsevier B.V.
doi:10.1016/j.jpowsour.2012.04.006

1. Experimental

Carbon cloth (CC, E-Tek, V2.02) and activated carbon cloth (ACC, Maxwell Tech.) were punched into small circular disks with an area of 1.27 cm^2 and used as the cathode current collector. Using phase inversion method [25], porous sulfur paper consisting of 90 wt.% sulfur and 10 wt.% binder was prepared by a general procedure as follows: Calculated amount of sulfur powder (>99.5%, Aldrich) was added to a 5 wt.% solution of Kynar FlexTM 2801, a poly(vinylidene fluoride-co-hexafluoropropylene) copolymer from Elf Atochem North America, dissolved in *N*-methyl pyrrolidinone, and ball-milled for 1 h to obtain a homogeneous slurry. The slurry was cast onto a glass plate using a doctor blade with a gap of 0.24 mm, followed by immersing the glass plate into a deionized water coagulation bath. Upon immersion, a yellow sulfur membrane (paper) was immediately floated out of the water. The sulfur paper was collected carefully, dried at 60 °C under vacuum for 2 h, and punched into 1.27 cm^2 circular disks. On average, the sulfur paper was measured to have a sulfur loading of 13 mg cm^{-2}. The liquid electrolyte was a solution consisting of 0.25 m $LiSO_3CF_3$ and 0.25 m $LiNO_3$ dissolved in a 1:1 (wt.) mixture of dimethyl ether (DME) and 1,3-dioxolane (DOL).

In a dry-room having a dew point of about −90 °C, the Li/S coin cells were assembled by stacking, in sequence, a Li foil, a Celgard® 3500 membrane, a sulfur paper, and a CC. Finally, 70 μL of liquid electrolyte was added from the back of CC, followed by placing a stainless steel disk on the CC as the contact space and sealing the cell. The Li/S cells were cycled on a Maccor Series 4000 cycler at 0.5 mA cm^{-2} in a voltage range between 1.7 V and 2.8 V. The charging process was controlled either by a cutoff voltage (2.8) or by a capacity equaling to 140% of the last discharge capacity, whichever came first. The purpose to add a capacity limit for the charging control is because upon the consumption of $LiNO_3$ on the Li anode, the Li/S cell or the Li/S cell without $LiNO_3$ cannot be charged up to the charge cutoff voltage [24,26,27].

2. Results and discussion

Fig. 1 shows the images of a highly porous sulfur paper made by the phase inversion method. Similar to those observed from the pure Kynar polymer membrane, the sulfur paper has relatively dense surface and highly porous body [25]. As an indication of the highly porous structure, the sulfur paper immediately gets wetted and swollen upon contact with any liquid electrolytes. Except for the high porosity, the sulfur paper is neither electronically conductive nor ionically conductive.

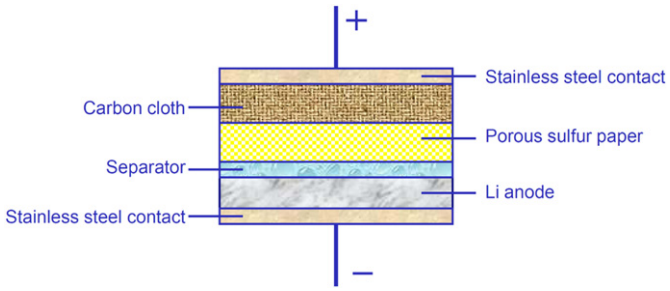

Fig. 2. Schematic configuration of the Li/S liquid cell.

Fig. 2 shows a schematic structure of the Li/S liquid cell, in which the cathode is composed of a CC layer and a sulfur paper. The CC layer not only serves as the cathode current collector but also provides the reaction sites for sulfur and PS species. According to the densities of sulfur and Li_2S, the volume of sulfur will expand to 1.66 times higher upon the complete reduction. Therefore, the voids in the woven textures of the CC can be used to accommodate the insoluble reduction products (Li_2S_2 and Li_2S) of the sulfur and PS. Here, the CC is unique in remaining the quite stable pores because of their fabric structure. The sulfur paper serves as the source of cathode active materials and allows the liquid electrolyte to soak in for the ionic conduction. In such a cell, the reactions of sulfur and PS are assumed to occur only on the CC surface.

Fig. 3 shows the voltage profile of the discharge and charge of the first cycle. From the viewpoint of phase transitions, the first discharge can be divided into the following four voltage regions:

Region I: A solid–liquid transition relates to the reduction from solid sulfur and small amount of the dissolved sulfur into dissolved high order PS (Li_2S_8). The formed PS anions are immediately dragged into the electrolyte by the electrical field of discharging process. With progressive discharging, the sulfur gradually "dissolves" into the electrolyte and the PS anions gradually migrate toward to the Li anode.

Region II: A liquid–liquid transition relates to the reductions from Li_2S_8 into varieties of soluble low order PS (Li_2S_x, $x \geq 4$). In this region, the dissolved Li_2S_8 functions as a liquid cathode (catholyte), and the voltage declines steeply with a decrease in the length of S–S chain. This step is affected greatly by the properties of electrolyte solvents, such as PS solubility and solution viscosity [26,27].

Region III: A liquid–solid transition relates to the reduction from the dissolved low order PS (Li_2S_4) into insoluble Li_2S_2 and Li_2S.

Region IV: A solid–solid transition relates to the reduction from the insoluble Li_2S_2 into insoluble Li_2S.

Among the above four voltage regions, Region III contributes to the major capacity of the sulfur cathode, and its capacity and

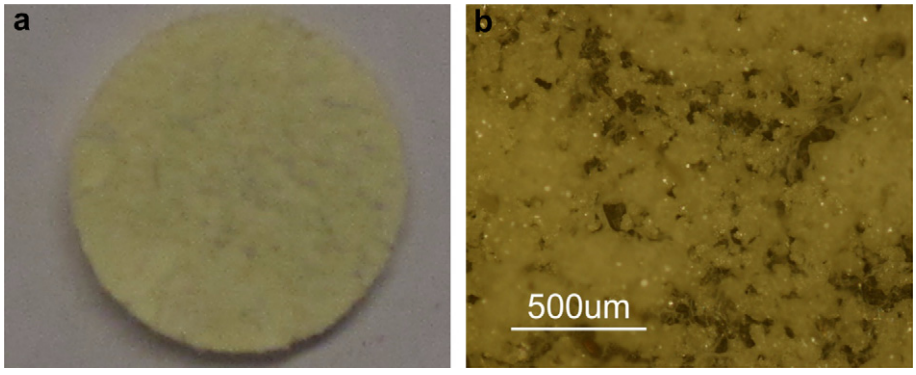

Fig. 1. Image of the porous sulfur paper made by phase inversion. (a) Photo by regular camera, and (b) Photo by optical microscopy.

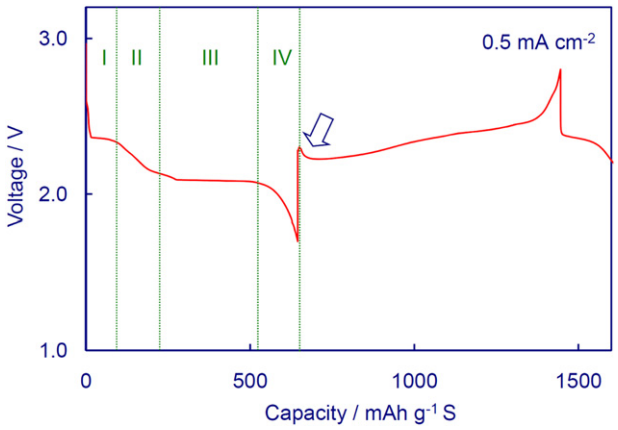

Fig. 3. Voltage profile of the first discharge and charge of a high capacity density Li/S liquid cell.

discharge voltage changes with the PS reduction products. When Li_2S is the predominant reduction product, the cell has higher capacity and slightly lower discharge voltages, whereas Region IV becomes shorter or even disappears. Due to the non-conductive nature of Li_2S_2 and Li_2S, Region IV is kinetically slow and normally suffers high polarization. For good discharge performance, Regions I–III require the PS having high solubility in electrolyte and the electrolyte having low viscosity, whereas Regions III and IV require the CC having high porosity to accommodate the final reduction products of sulfur.

In charging process, the voltage shows a small drop in very beginning, as indicated by the arrow in Fig. 3. This voltage drop can be attributed to the chemical dissolution (oxidization) of Li_2S and Li_2S_2 by the high order PS formed in the very beginning of charging process, as described by Eqs. (1) and Eq.(2), where (x − y) and (1 + y) are greater than 2:

$$Li_2S_x + Li_2S \rightarrow Li_2S_{x-y} + Li_2S_{1+y} \quad (1)$$

$$Li_2S_x + Li_2S_2 \rightarrow Li_2S_{x-y} + Li_2S_{2+y} \quad (2)$$

These two reactions bring the insoluble Li_2S and Li_2S_2 into liquid system, which have been known to contribute to the reversibility of Li/S cells [26,27].

Fig. 4 shows the discharge capacity and cycling efficiency of the Li/S liquid cell. The cell starts with an initial capacity of 645 mAh g^{-1} S. This low initial capacity suggests that sulfur in the sulfur paper may not be fully utilized in the first discharge. The residual sulfur can be utilized in the subsequent cycles or directly dissolved into the solution by the low order PS through the similar reactions as occurred in the preparation of lithium polysulfide solutions [22,24]. In the present cells, the porosity of CC and the dissolution capacity of PS in the electrolyte are two major factors to determine the cell's capacity. In subsequent cycles, the capacity declines slowly with cycle number, which can be attributed to the progressive decrease in the cycling efficiency. As indicated in Fig. 4, the cycling efficiency progressively declines with cycle number from the maximum of 95.4% at 3rd cycle to 71.4% at 21st cycle, then the cycling efficiency remains constantly. Here, the 71.4% value is pre-set by the charging schedule, and it equals to the reciprocal of 140%. This means that once the cycling efficiency declines to 71.4%, the charge process is no longer controlled by the cutoff voltage, instead, terminated by the pre-set capacity, i.e., 140% of the last discharge capacity.

In order to understand the low charging efficiency, the discharge and charge voltage curves of the 5th and 25th cycles are plotted in Fig. 5. It is shown that the charging voltage at 5th cycle reaches the cutoff voltage (2.8 V), and that the charging process is terminated by the pre-set cutoff voltage. However, the charging voltage at 25th cycle stays at 2.42 V until the charging process is terminated by the capacity limit, showing severe redox shuttle reactions of the dissolved PS. This is because upon cycling, $LiNO_3$ is gradually depleted on the Li anode so that the Li anode loses the protection from the reactions by the oxidative PS anions. The results above indicate that $LiNO_3$ is not sufficient to protect the Li anode in the high capacity density Li/S liquid cells although it could be the most effective additive reported ever for the rechargeable Li/S cells [24,28–30]. Therefore, the electrolyte having more effective protection of the Li anode against the highly concentrated PS solution is needed for long cycle life of the high capacity density Li/S liquid battery.

On the porous carbon electrode, two types of woven carbon clothes, as summarized in Table 1, are compared for the purpose of demonstration. The CC has low surface area (BET specific surface area = 3.67 m^2 g^{-1}), which was treated with Telfon® for application in the gas diffusion layer of proton exchange membrane fuel cells, whereas the ACC has high surface area (871.4 m^2 g^{-1}), which was impregnated with aluminum particles for use in electric double layer capacitor [31]. The effects of these two carbon clothes on the first discharge of Li/S liquid cells are presented in Fig. 6, showing that the ACC gives higher overall capacity than the CC although it has relatively lower area porosity (i.e., 17.5 cm^3 cm^{-2} vs. 20.2 cm^3 cm^{-2} of the CC). This is probably because the ACC offers more reaction sites for the reductions of the dissolved PS, which is attributed to its higher surface area. The result above also suggests

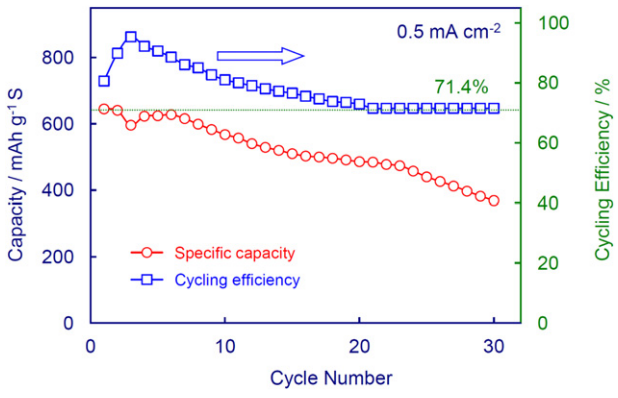

Fig. 4. Discharge capacity and cycling efficiency of a Li/S liquid cell, recorded at 0.5 mA cm^{-2} between 2.5 V and 2.8 V.

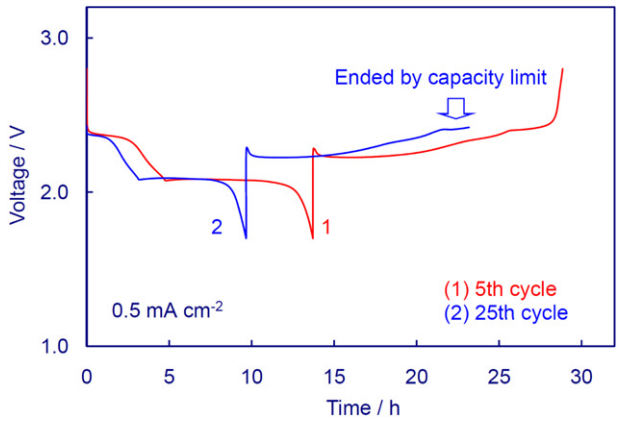

Fig. 5. Voltage curves of a Li/S liquid cell at 5th and at 25th cycle, respectively.

Table 1
Basic physical properties of carbon clothes.

	Carbon cloth	Activated carbon cloth
Thickness, mm	0.25	0.30
BET surface area, $m^2\ g^{-1}$	3.67	871.4
Area density, g cm^{-2}	18.5	13.9
Area porosity, $cm^3\ cm^{-2}$[a]	20.2	17.5
Capacity of 1st discharge, mAh g^{-1} S	645	778

[a] Porosity was measured using solution adsorption method as described in Ref. [32].

that not all pores in the CC texture can be filled by the PS reduction products, instead, only those capable of serving as the reaction sites can be filled. This phenomenon is very similar to those observed from the Li/air cells where the cathode reduction products are Li_2O_2 and Li_2O [32].

Fig. 7 compares the effect of carbon cloth on the capacity retention of the Li/S liquid cells. When the ACC is used, the initial capacity of sulfur increases to 778 mAh g^{-1} S, equaling to an area capacity density of 10.1 mAh cm^{-2} CC, which could be the highest capacity density among the rechargeable Li/S cells reported ever. However, the use of ACC cannot suppress capacity fading. As shown in Fig. 7, the cells with ACC and CC have similar capacity fading rates.

Since the sulfur eventually dissolves, in the form of PS, into liquid electrolyte in the first discharge, the initial mixing state of sulfur and carbon in the cathode of the Li/S liquid cells is not important. In further development, the porous sulfur layer can be directly applied onto the surface of carbon cloth by melt-spray or melt-immersion for a binder-free cathode, and the carbon cloth can be optimized in terms of the texture (for example, woven and non-woven), thickness, porosity, specific surface area and carbon fiber diameter.

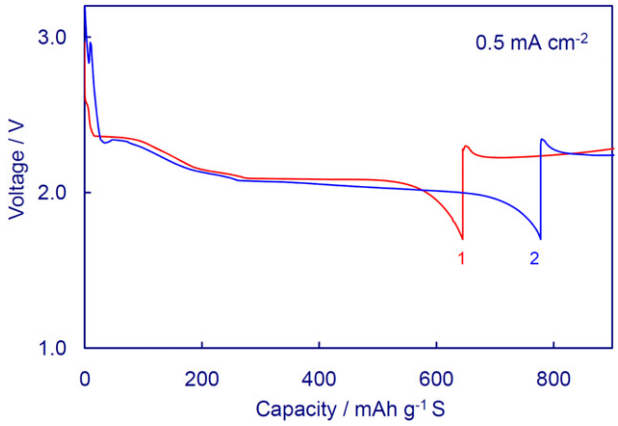

Fig. 6. Effect of carbon cloth on the capacity of the first discharge of Li/S liquid cells. (1) Carbon cloth, and (2) Activated carbon cloth.

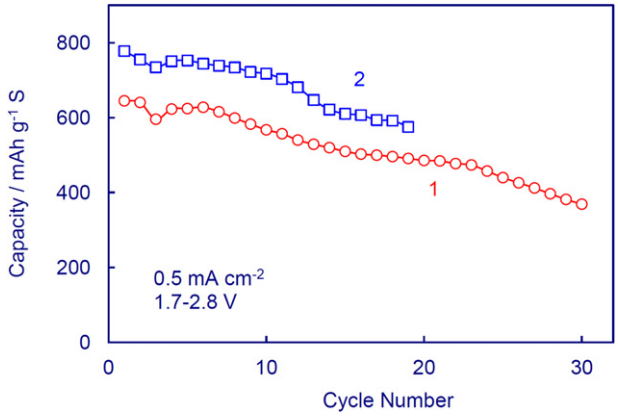

Fig. 7. Comparison of capacity retention for Li/S liquid cells with different carbon clothes. (1) Carbon cloth, and (2) Activated carbon cloth.

3. Conclusions

This work demonstrates that the rechargeable Li/S liquid cells having exceptionally high capacity density can be made by starting with a high sulfur loading cathode. Initial mixing state of the sulfur and carbon in the cathode is not important as the PS active species eventually dissolve into liquid electrolyte. For a cell with sufficient amount of sulfur, its capacity is determined by the porosity of carbon electrode and the dissolution capability of PS in liquid electrolyte while the cycle life is determined by the cycling efficiency of the Li anode. Future improvement can be placed on (1) the carbon electrode having high surface area and porosity, (2) the liquid electrolyte having high PS solubility, and (3) the protection of Li anode against highly concentrated PS solution.

Acknowledgments

The authors would like to thank Dr. R.Z. Jiang of the fuel cell team for supplying carbon cloth.

References

[1] Y.V. Mikhaylik, J.R. Akridge, J. Electrochem. Soc. 151 (2004) A1969.
[2] V.S. Kolosnitsyn, E.V. Karaseva, Russ. J. Electrochem. 44 (2008) 506.
[3] J.L. Wang, J. Yang, J.Y. Xie, N.X. Xu, Y. Li, Electrochem. Commun. 4 (2002) 499.
[4] Y.J. Choi, Y.D. Chung, C.Y. Baek, K.W. Kim, H.J. Ahn, J.H. Ahn, J. Power Sources 184 (2008) 548.
[5] C. Lai, X.P. Gao, B. Zhang, T.Y. Yan, Z. Zhou, J. Phys. Chem. C 113 (2009) 4712.
[6] X. Ji, K.T. Lee, L.F. Nazar, Nat. Mater 8 (2009) 500.
[7] C. Liang, N.J. Dudney, J.Y. Howe, Chem. Mater. 21 (2009) 4724.
[8] B. Zhang, C. Lai, Z. Zhou, X.P. Gao, Electrochim. Acta 54 (2009) 3708.
[9] L. Yuan, H. Yuan, X. Qiu, L. Chen, W. Zhu, J. Power Sources 189 (2009) 1141.
[10] C. Wang, J. j. Chen, Y.N. Shi, M.S. Zheng, Q.F. Dong, Electrochim. Acta 55 (2010) 7010.
[11] B. Zhang, X. Qin, G.R. Li, X.P. Gao, Energy Environ. Sci. 2 (2010) 1531.
[12] J.Z. Wang, L. Lu, M. Choucair, J.A. Stride, X. Xu, H.K. Liu, J. Power Sources 196 (2011) 7030.
[13] H. Wang, Y. Yang, Y. Liang, J.T. Robinson, Y. Li, A. Jackson, Y. Cui, H. Dai, Nano Lett. 11 (2011) 2644.
[14] N. Jayaprakash, J. Shen, S.S. Moganty, A. Corona, L.A. Archer, Angew. Chem. Int. Ed. 50 (2011) 5904.
[15] J. Guo, Y. Xu, C. Wang, Nano Lett. 11 (2011) 4288.
[16] R. Elazari, G. Salitra, A. Garsuch, A. Panchenko, D. Aurbach, Adv. Mater 23 (2011) 5641.
[17] S.R. Chen, Y.P. Zhai, G.L. Xu, Y.X. Jiang, D.Y. Zhao, J.T. Li, L. Huang, S.G. Sun, Electrochim. Acta 56 (2011) 9549.
[18] S.E. Cheon, K.S. Ko, J.H. Cho, S.W. Kim, E.Y. Chin, H.T. Kim, J. Electrochem. Soc. 150 (2003) A800.
[19] H.S. Ryu, H.J. Ahn, K.W. Kim, J.H. Ahn, J.Y. Lee, J. Power Sources 153 (2006) 360.
[20] Y.J. Choi, K.W. Kim, H.J. Ahn, J.H. Ahn, J. Alloys Compounds 449 (2008) 313.
[21] J.J. Chen, X. Jia, Q.J. She, C. Wang, Q. Zhang, M.S. Zheng, Q.F. Dong, Electrochim. Acta 55 (2010) 8062.
[22] R.D. Rauh, K.M. Abraham, G.F. Pearson, J.K. Surprenant, S.B. Brummer, J. Electrochem. Soc. 126 (1979) 523.
[23] H. Yamin, A. Gorenshtein, J. Penciner, Y. Sternberg, E. Peled, J. Electrochem. Soc. 135 (1988) 1045.
[24] S.S. Zhang, J. Read, J. Power Sources 200 (2012) 77.
[25] S.S. Zhang, K. Xu, D.L. Foster, M.H. Ervin, T.R. Jow, J. Power Sources 125 (2004) 114.
[26] S.S. Zhang, J. Electrochem. Soc., in press.
[27] S.S. Zhang, Electrochim. Acta, in press, http://dx.doi.org/10.1016/j.electacta.2012.03.081.
[28] Y.V. Mikhaylik, U.S. Patent (2008) 7,352,680.
[29] D. Aurbach, E. Pollak, R. Elazari, G. Salitra, C.S. Kelley, J. Affinito, J. Electrochem. Soc. 156 (2009) A694.
[30] X. Liang, Z. Wen, Y. Liu, M. Wu, J. Jin, H. Zhang, X. Wu, J. Power Sources 196 (2011) 9839.
[31] C.J. Farahmandi, J.M. Dispennette, U.S. Patent 5,777,428 (1998).
[32] S.S. Zhang, D. Foster, J. Read, J. Power Sources 195 (2010) 1235.